Relaxation of Second-Harmonic Generation in Guest/Host Polymers Poled by Indium-Tin Oxide Sandwich Electrodes

Stephan Schüssler, Ranko Richert,*,† and Heinz Bässler

Fachbereich Physikalische Chemie und Zentrum für Materialwissenschaften, Universität Marburg, 35032 Marburg, FRG

Received February 28, 1994; Revised Manuscript Received May 2, 1994®

ABSTRACT: Second-harmonic generation (SHG) is used to monitor reorientation dynamics of 4-(dimethylamino)-4'-nitrostilbene doped at 1 wt % in poly(ethyl methacrylate) within a temperature range of $T_G \pm 30$ K. Special emphasis is put on a systematic analysis of experimental conditions and their severe impact on SHG data for samples which are poled in an indium-tin oxide (ITO)-sandwich-electrode configuration. These effects include thermal history, local heating effects due to laser focus, importance of dopant concentration, physical aging, details of the poling procedure, and charge-injection effects. The fast initial response of the SHG signal upon field switching is attributed to space charge effects. We show how the problem of SHG reproducibility can be overcome with appropriate experimental conditions. Analysis of the reliable data is based on a Gaussian distribution of energy barriers for the dopant relaxation which yields superior fits compared to a stretched exponential function. The Arrhenius-like behavior of the mean SHG decay rate points toward a decoupling of the dopant motion from the bulk α-process of the polymer host. Additionally, a novel repoling technique and its implications are discussed.

Introduction

Intense research efforts are in progress aiming at the development of polymeric materials exhibiting large nonlinear optical (NLO), especially electrooptic and second-harmonic generation (SHG), activity.[1,2] Such materials bear interesting potential applications as optical switches, filters, waveguides, and frequency-doubling devices. Organic molecules possessing a large conjugated π-electron system terminated by strong acceptor and donor groups show high values of the second-order polarizability β. During the last decade it has been shown that incorporating such molecules into an amorphous polymer by various methods is a very promising approach in this area of research.[3-5] In doing so one is able to combine the desired electrooptical properties with the technical quality and versatility of a polymer compound. Due to the fact that such an isotropically doped polymer lacks a $\chi^{(2)}$ activity, a common method to introduce these NLO effects is to apply a strong dc poling field to the sample in order to break the symmetry by aligning the dopants. Besides thermal stability and other physical and mechanical properties the usefulness of a particular material is decisively determined by the temporal stability of the polar orientation of the chromophores.

Based on the fact that a poled polymer is inherently in a nonequilibrium state, the long-term stability at convenient temperatures is very important for technical applications. Orientational relaxation after removing the poling field arises from thermal reorientational effects being strongly dependent on the rotational mobility in the glassy system. Important parameters in this context are absolute temperature, molecular structure of both the polymer and the chromophore, and the amount of the so-called free volume. The latter quantity depends critically on the temperature relative to the glass transition temperature T_G which determines the liquid to solid transition of amorphous systems. One main aspect relevant to applications is to prevent this relaxation, as was recently done by employing doped precurser polymers which can be cross-linked either thermally or photochemically.[6] A different route is the use of thermally extraordinarily stable polymer/chromophore systems combined with very high values of the glass transition.[7,8] The situation is complicated by the fact that the nature of the relaxational behavior of these systems with regard to poling conditions and different kinds of possible molecular motions is presently not fully understood and still a matter of controversy.

The SHG technique is selectively sensitive to the dopant rotational mobility because SHG features are strictly associated with a nonrandom orientation of the chromophores. Using the free gas approximation, the related tensor elements of the macroscopic second-order susceptibility $\chi^{(2)}$ are expressed by:

$$\chi^{(2)}_{333} = NF\beta_{zzz}\langle\cos^3\theta\rangle \quad (1)$$

$$\chi^{(2)}_{311} = {}^1/_2 NF\beta_{zzz}(\langle\cos\theta\rangle - \langle\cos^3\theta\rangle) \quad (2)$$

where N is the number of chromophores and F is a dimensionless combined field factor of the electric and electromagnetic fields involved. μ denotes the ground-state dipole moment of the active species, E is the dc poling field, and β_{zzz} represents the tensor element of molecular hyperpolarizibility along the dipole axis. The subscripts 1 and 3 refer to the "macroscopic coordinates", whereas z indicates the molecular dipole axis ("microscopic coordinates"). θ represents the angle between the z and 3 direction.

Evaluating these expressions via the first- and third-order Langevin functions and making use of the low-field approximation leads to:

$$\chi^{(2)}_{333} = NF\beta_{zzz}(\mu E/5kT) \quad (3)$$

$$\chi^{(2)}_{311} = NF\beta_{zzz}(\mu E/15kT) \approx \chi^{(2)}_{333}/3 \quad (4)$$

For a p-polarized fundamental beam with electric field E_ω

† Present address: Max-Planck-Institut für Polymerforschung, Ackermannweg 10, 55128 Mainz, FRG.

® Abstract published in *Advance ACS Abstracts*, June 1, 1994.

0024-9297/94/2227-4318$04.50/0

and the 1–3 plane as the plane of incidence, the NLO polarization at 2ω is given by:

$$P^{p}_{NL} \propto \begin{cases} \chi^{(2)}_{311} E_\omega \cos\phi_\omega E_\omega \sin\phi_\omega \\ 0 \\ {}^1/_2(\chi^{(2)}_{311} E_\omega^2 \cos^2\phi_\omega + \chi^{(2)}_{333} E_\omega^2 \sin^2\phi_\omega) \end{cases} \quad (5)$$

where ϕ_ω denotes the internal angle of incidence.

Thus it becomes clear that the square root of the SHG intensity which is proportional to the nonlinear polarization depends on the average orientation of the dopants expressed via $\langle\cos\theta\rangle$. A detailed survey of the theory roughly outlined above is given elsewhere.[1-3,9]

Our main concern is the factors which affect the relaxation process of the mean chromophore orientation which we monitor via the decay of the SHG signal. In this respect it is desirable to start the study with a system of moderate complexity. Thus, in order to prevent correlations among the chromophore moiety, low dopant concentrations are used. Furthermore, the preferred method of incorporating the dye is homogeneously doping the polymer matrix, which leads to the so-called guest/host systems. In such systems the NLO chromophores are dissolved homogeneously in low concentrations in an amorphous polymer instead of having active side groups or active chain segments. Excellent agreement with the above-mentioned theory has been achieved recently using guest/host systems.[10] In contrast to other methods such as dielectric relaxation spectroscopy, which probes the bulk polymer, the SHG technique is selectively sensitive to the dopant orientation and therefore to the dopants' microenvironment. Using the SHG technique the chromophore orientation can be monitored continuously in situ over a wide range of time scales and temperatures. In contrast to several other relaxation experiments, the SHG method has the advantage that a completely random orientation is unambiguously identified by the absence of the SHG activity.

A large body of efforts is reported in the literature which aim at understanding the molecular processes of such systems by analyzing the decay curves of the SHG signal after switching off the external electric field.[11-13] Recently, the experimental time range has been expanded into the microsecond domain.[10,14] A common route in describing such SHG decay data[15,16] has been a single Kohlrausch–Williams–Watts (KWW) or stretched-exponential pattern given by:[17]

$$g(t) = A \exp[-(t/\tau)^\beta] \quad (6)$$

where β ($0 < \beta \leq 1$) is a measure of the deviation from pure exponentiality and τ is a characteristic relaxation time. Alternatively, biexponential functions[18,19] and a superposition of two KWW decays[13] have also been used, all of which are empirical approaches. Additional ambiguity regarding the decay pattern stems from the use of the corona poling technique which is notorious to affect the SHG response function in an unpredictable manner.[13,18] The literature in this field demonstrates that discrepancies in the results and their evaluation are encountered, even when working with very similar materials.[13] Although reliable data are a prerequisite of a sensible data analysis and interpretation, the reproducibility is a severe problem of SHG relaxation experiments.[20] Therefore, a careful investigation of the necessary experimental conditions for a satisfactory data quality seemed highly desirable.

In this study we report on experimental results of SHG data obtained for electrode poled poly(ethyl methacrylate) (PEMA) films doped with 4-(dimethylamino)-4′-nitrostilbene (DANS). After carefully optimizing the experimental conditions, our data showed excellent reproducibilities over an expanded temperature range near T_G not reported before. The data can be fitted well on the basis of a Gaussian distribution of the logarithm of dopant reorientation rates. Another promising approach with regard to the interpretation of the decay process is based on results of SHG data gained from realignment traces recorded directly after an incomplete SHG signal relaxation.

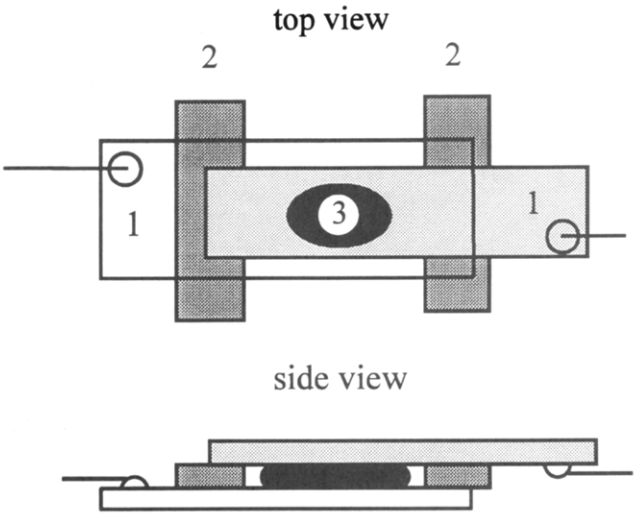

Figure 1. Design of the sample cell for poling guest/host polymers in the sandwich electrode configuration. Various slide sizes and arrangements were used to prevent electrical breakdown: (1) ITO slide, (2) Kapton sheet, (3) sample.

Experimental Section

1. Sample Preparation. Appropriate amounts of DANS (Kodak or alternatively preparable via the Wittig reaction[21]) and PEMA ("Elvacite 2043", DuPont; M_w = 44 000, M_n = 29 000) were dissolved in HPLC-grade chloroform (Aldrich) to form a solution of 1 wt % chromophore concentration. PEMA was dried previously for 3 days in vacuum at 120 °C to remove possible low molecular weight impurities. Some drops of this solution were cast on a indium–tin oxide (ITO)-coated glass ("Baltracon 417", Balzers). The sample was dried at elevated temperatures (≈50 °C) for 30 min and then under vacuum for 12 h at 45 °C; a second drying step followed under high vacuum for a further 12 h at 25 °C. Drying at temperatures significantly higher than 50 °C as well as using dichloromethane as the solvent supported aggregation of the chromophores which is easily detected using crossed polarizers in a microscope. Dried samples ($T_G \approx 62$ °C measured via DSC at a heating rate of 10 K/min) were heated up to about 150 °C, and a second ITO slide was carefully pressed on top of the first one using spacer sheets (Kapton, DuPont; thickness 25 ± 1 μm) in order to maintain a well-defined temperature-invariant thickness of the films. By applying this new technique, we were able to prepare homogeneous films of excellent optical quality and high reproducibility. These sandwich cells had a capacity of approximately 100 pF. The use of transparent ITO electrodes allows measurement in transmission mode albeit using electrode poling instead of a corona discharge. Due to higher accessible fields, the latter possibly offers an enhanced alignment of dopants, its disadvantage being residual surface charges whose influence on the signal decay can hardly be quantified or reproduced.[11,18] Mechanically stable electrical connections were affixed using a silver–epoxy resin (Epoxy-Produkte, Fürth, FRG). The design of the sample cell is shown in Figure 1.

2. Poling and Thermal Erase. Prior to each measurement the built in sample was heated up to 160 °C, poled for 10 min with a dc field of (−)0.14 MV/cm. Then the field was switched off, and the thermal history of the film was erased by maintaining 160 °C for 1 h (thermal erase) before quenching down to the

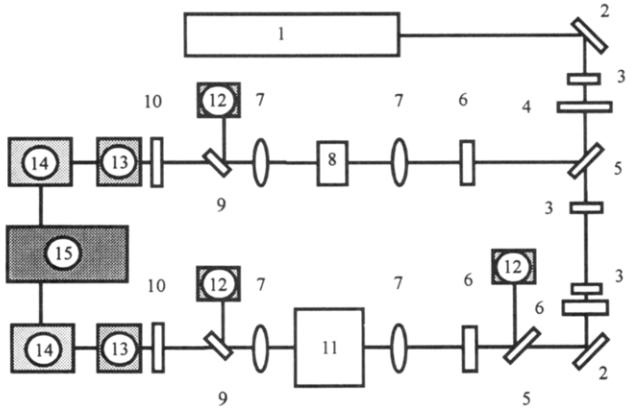

Figure 2. Schematic representation of the experimental setup: (1) Nd:YAG laser, (2) mirror, (3) polarizer, (4) chopper, (5) beam splitter, (6) λ/2 plate, (7) lens, (8) quartz reference, (9) IR filter, (10) filter, (11) sample, (12) photodetector, (13) PMT, (14) lock-in amplifier, (15) personal computer.

poling temperature of 90 °C ($\simeq T_G + 30$ K) within 85 s by means of an enforced air flow. Allowing for a period of 15 min of thermal equilibration, the poling field of 0.14 MV/cm (cf. low-field approximation) was applied and maintained for 60 s before the sample was cooled down to the desired temperature of relaxation within ≈1 min. After a further 5 min of thermal equilibration the field was switched off while simultaneously shorting the electrodes to remove any possible surface charges.

On the basis of a large amount of preliminary experiments, we have empirically established the above procedure which turned out to yield highly reproducible results regarding the SHG decay pattern. The criteria for this optimization were minimizing the initial fast "switching effect" combined with a high SGH efficiency (see below). Especially in the case of a long-time relaxation study (possibly combined with physical aging under an applied field) only a thermal erase at such high temperatures and expanded time scales led to reproducible results. Concerning the reproducibility, it was important that this procedure could be repeated within an accuracy of better than 5% with respect to time. Poling with higher field strengths did not improve the signal quality but rather resulted in an enhanced danger of electrical breakdown.

3. Detector Setup. The experimental setup is depicted schematically in Figure 2. The laser fundamental beam at 1064 nm is generated by a mode-locked (76 MHz) Nd:YAG laser (Quantronix 416). The beam is p-polarized and split, so that a frequency-doubled reference signal of a y-cut quartz single crystal can be measured simultaneously. Photomultiplier tubes (PMT) with a narrow band interference filters are used to detect the second-harmonic signal at 532 nm. PMT output signals are acquired using the lock-in technique in combination with an external chopper blade operated at 730 Hz. The reference path allowed for obtaining data with on-line normalization to the quartz standard. The laser power incident on the sample was checked before starting each measurement. In order to work at known intensity conditions, the transmitted intensities of the fundamental beam were also monitored continuously in both the signal and the reference path. The software especially designed to drive this experiment allows one to record each set of data at up to a 40-Hz sampling rate. Possible phase drifts of the lock-in signal and offsets where checked and considered prior to and after each experiment so that scans subject to the risk of base-line drifts could be rejected. The selected time constants and filter roll-off parameters of the lock-in amplifier were also checked to insure that decay traces are not bandwidth limited. A severe change in dopant concentration due to diffusion or local bleaching at these temperatures was not observed. All data presented below is shown with the signal-to-noise ratio as originally acquired.

Results and Discussion

1. Heating Effects. In the course of reproducibility tests, experiments with different samples under constant experimental conditions were carried out. Thereby a remarkable dependence of SHG decay kinetics on the extent of laser focusing on the sample was noted. Considering a 76-MHz repetition rate with an estimated pulse energy of 20 nJ and an averaged pulse width of 250 ps, sample heating has to be considered. Due to fundamental problems with the input coupling, it was not possible to use an acoustooptomodulator (AOM) cell to enlarge the intervals between each pulse. Therefore, a special blade for the 730-Hz chopper with a 1:8 duty cycle was manufactured in order to reduce the average incident laser power. Successive defocusing at a constant power of the fundamental beam in the sample channel led to slower kinetics until no further effects of the spot size could be detected. As outlined in Figure 3, an excellent reproducibility was also obtained for this limit of low irradiation power. The following experiments were done in a manner which rules out such heating effects.

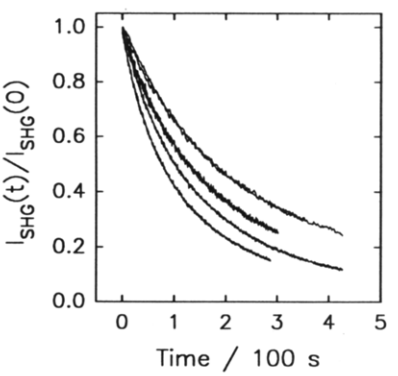

Figure 3. Influence of the laser focus on the SHG decay kinetics measured at T = 70 °C. Coincident upper curves indicate compensation of the effect.

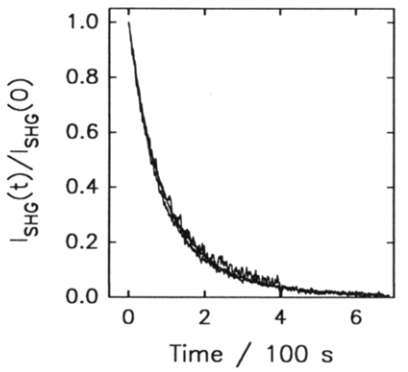

Figure 4. Effect of using different samples and doubling the dopant concentration from 0.5 to 1 wt % DANS in PEMA at T = 70 °C.

2. Concentration Effects. Bearing in mind a minimized interaction among the chromophores, further measurements were made in order to examine how dopant concentration affects the SHG relaxation of a given system. We found that, apart from a poor signal-to-noise ratio, a sample of 0.5 wt % DANS shows the same kinetic behavior compared to a sample of twice the chromophore content. However, preparing films doped with significantly more than 1 wt % DANS resulted in aggregation phenomena. Figure 4 shows the normalized data of three samples of identical material with different chromophore concentrations analyzed under comparable conditions. These results undoubtedly rule out any significant impact of the dopant concentration on the normalized SHG decay when working with up to 1 wt % doped material.

3. Effects due to Space Charges, Traps, and Impurities. For all the experiments—even with different samples—a common feature was detected when switching the field: A very fast *increase or decrease* of the SHG

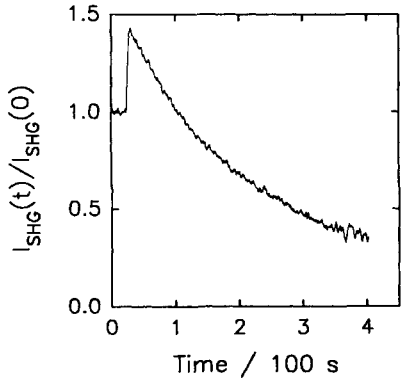

Figure 5. Raw data of a relaxation experiment with a large switching effect for a 1 wt % DANS in PEMA sample at $T = 70$ °C.

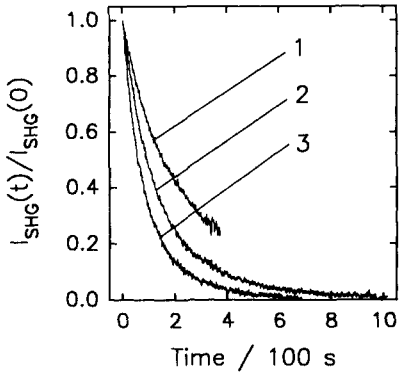

Figure 6. Influence of the switching effect on normalized relaxation data for 1 wt % DANS in PEMA at $T = 70$ °C. Curve 1 refers to 40%, curve 2 to 15%, and curve 3 to 8% relative contribution to the SHG signal of the fast response to switching the external field.

signal of varying amplitude was observed. Figure 5 shows this feature for a typical set of raw data. On the basis of low-temperature (sub-T_G) measurements, we found that this switching effect was not temperature dependent within our resolution. Investigations while always using the very same sample spot lead to the conclusion that repeated application of the thermal erase and poling procedure did affect the extent of this response. As can be seen in Figure 6, a small "switching effect" is in all cases correlated with an accelerated orientational relaxation. Furthermore, the extent of this switching effect was found to be influenced by irradiation with light of 300–450 nm (typical values are 5-min irradiation with a 100-W halogen lamp at $\simeq$100 °C). The resulting irradiation-induced decrease of the effect again led to faster decay kinetics. We also observed that the switching effect does not affect the kinetics at all as long as its contribution to the SHG signal does not exceed 10% in either direction. Since instantaneous SHG signal changes in excess of 10% were paralleled by a slowing down of the orientational response and by low SHG efficiencies, decay traces which exhibit a higher switching effect will be disregarded in the following.

When examining this effect at sub-T_G temperatures, we often obtained decay curves implying a fast process followed by a second much slower relaxation. Some authors[10,13,14,19] have also reported very fast decay processes right after switching off the field, similar to the effect described above. Dhinojwala[10,14] attributed this feature to a nonlinear effect of higher order with coefficient γ, writing $\chi^{(2)}$ as the sum of two terms:

$$\chi^{(2)} \propto E(\gamma + \mu\beta/5kT) \qquad (7)$$

According to this model, γ quantifies an instantaneous contribution since the electric-field-induced third-harmonic generation term is insensitive to the average chromophore orientation. In our experiments, however, we observed a fast *rise* of the SHG signal as a rule and a fast decay as an exception only. Such an *increase* of the SHG signal when removing the field obviously does not comply with the interpretation given by Dhinojwala. On the other hand, the fast SHG response of varying sign might consist of a rise of ambiguous origin and a decay which stems from the γ term in eq 7. In our opinion, however, all the observed characteristics of our switching effect underline the statement that space charges are an additional important factor to be considered when discussing SHG decay kinetics. We thereby agree with other authors that this fast process should not reflect any changes in dopant reorientation.

4. Charge-Injection Effects. In order to gain a more quantitative understanding of the poling process, a series of poling experiments with simultaneous current measurements were carried out. The cell current was recorded via the voltage drop across a 100-kΩ resistor in series with the cell using a Keithley 195A digital multimeter. A general characteristic observed during the poling process was an immediate current of the order 10–40 nA (depending on the voltage applied) when poling at $T = 90$ °C. When the sample was cooled to the desired relaxation temperature, a steady decrease in current by up to 1 order of magnitude could be seen. According to the SHG signal, the corresponding dopant alignment has almost saturated after 1 min at $T = 90$ °C. The thermal quenching was accompanied by an increasing SHG value as expected on the basis of $\chi^{(2)} \propto 1/kT$ (see eq 3). Having reached the relaxation temperature, the current always started rising again by a factor of $\simeq$3 and reached a steady-state value on a time scale of several hours (typically 4–6 h). This behavior was parallelled by a decreasing SHG signal, yet with a similar temporal pattern. The shape of the SHG decay under field was found to depend on the sample history: Samples which had been kept under field for hours in a previous poling cycle were found to be less sensitive to poling (typically one-third of the expected SHG signal strength), although the remaining experimental conditions had not been altered and a 1 h thermal erase process at 160 °C had been carried out. Figure 7 shows current and SHG signal traces of a representative experiment.

Comparing normalized decay data from experiments in which the relaxation had been started immediately after thermal quenching and those in which steady-state conditions under field have been achieved prior to removing the field yielded excellent coincidence for $T \geq T_G$. Apart from demonstrating the capabilities of the apparatus, these results give evidence that the observed slow signal decay under field is not related to any additional changes of orientation effects concerning the matrix material. If this were the case, one would expect a significant difference in the SHG traces for these two conditions.

At this time we postulate that an injection process from one of the ITO electrodes is responsible for these phenomena. Apparently, injected charges are sufficiently mobile at high temperatures to follow the dipole movements without affecting the dopant's kinetics. Vestweber[22] has also recently reported about similar ITO charge injection in the course of designing polymer LEDs. Such an interpretation would agree with the observed signal decay under field since injected charges migrating through

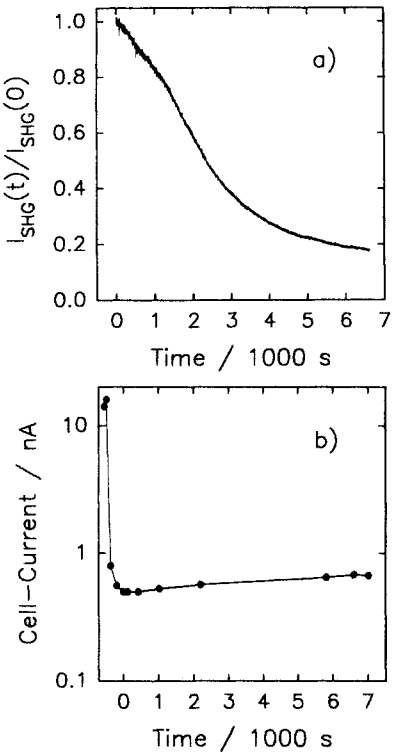

Figure 7. Temporal progress of the SHG signal (a) and corresponding cell current (b) of a PEMA sample doped with 1 wt % DANS. Data are obtained at $T = 40$ °C ($\approx T_G$ -20 K) and for a poling field of $E = 0.108$ MV/cm. $t = 0$ refers to the start of SHG signal registration.

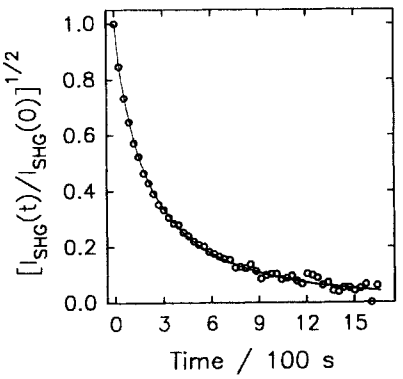

Figure 8. SHG relaxation of a PEMA sample doped with 1 wt % DANS at $T = 70$ °C including the fit based on the Gaussian density of barriers. Experimental data (circles) have been sampled at a rate of 4 Hz. Only 1 out of 150 data points is shown for clarity.

the sample would seriously affect the local field in the sample and weaken the effective field. Effects of inhomogeneous charge densities have to be considered as well because our experiment probes only a small amount of the sample volume. Additionally, the charges within the sample are not necessarily influenced by a thermal erase cycle and therefore can influence subsequent measurements. These results emphasize that the electrode material might affect the relaxation pattern significantly. However, our experimental conditions are adjusted to minimize charge injection effects regarding the normalized relaxation kinetics. It should be noted that there is no indication for a direct correlation of the above phenomenon to the previously described switching effect, suggesting that the latter is due to deeply trapped space charges.

5. Temperature Dependence of the SHG Decay. Figure 8 shows typical SHG relaxation data of PEMA doped with 1 wt % DANS. The investigated temperature

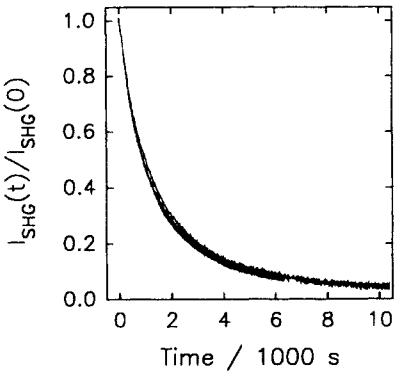

Figure 9. Representative quality of reproducibility of decay data of a PEMA sample doped with 1 wt % DANS at $T = 50$ °C ($=T_G$ - 10 K). The three measurements were independently recorded within a period of 3 weeks.

range covers $T_G \pm 30$ K. The vertical axis represents the square root of the normalized SHG intensity and is thus proportional to the average dopant orientation. Therefore, evaluation of this data should yield information about the chromophore motion in both the glassy and the rubbery state of the matrix. All the measurements correspond to the optimized experimental situations outlined above. Based on these conditions and on the degree of reproducibility achieved here, these experiments should be regarded as being highly reliable. As an example Figure 9 shows three independent measurements at T_G - 10 K.

Regarding a quantitative description of the relaxation process as a function of time, single-exponential as well as KWW fits gave no satisfactory results. A different model based on a Gaussian distribution of energy barriers for the elementary events turned out to be more appropriate in terms of fit quality. Within this model the rate ν of a particular first-order process subject to the barrier $\epsilon = E_A/kT$ is determined by the Arrhenius expression $\nu = \nu_0 e^{-\epsilon}$. The corresponding ensemble-averaged decay for a Gaussian probability density of width σ for finding a site related to ϵ is given by

$$M(t) = \frac{1}{\sigma(2)^{1/2}\pi}\int_{-\infty}^{\infty} \exp[-\epsilon^2/2\sigma^2 - \nu_0 e^{-\epsilon}t]\, d\epsilon \qquad (8)$$

This scheme has already been successfully applied to describe the kinetics of photoisomerization[23-25] in similar matrix materials and actually stems from the model of parallel relaxing species in disordered materials. Thereby, its background differs strongly from the KWW approach which is rather related to serial or hierarchical processes.[26] For amorphous systems the particular choice of a Gaussian distribution of ϵ can be motivated by the central limit theorem. Using the Gaussian density of barriers for fitting normalized data, only two fit parameters are involved: first, the slope of the normalized decay at $t = 0$ which can be identified as the mean rate $\langle\nu\rangle = \nu_0 \exp(\sigma^2/4)$ of the entire relaxation process and, second, the dispersion parameter σ describing the width of the distribution of the logarithm of rates. The latter quantity thus takes into account the effect of disorder on the overall process. Details concerning this model are available elsewhere.[24] Based on the good coincidence of the fit and experimental data, this model turns out to serve as an excellent tool to describe the relaxation data, at least from an empirical point of view.

Figure 10 shows the temperature dependence of the dispersion of $\ln(\tau)$ extracted from data obtained under isothermal conditions. As is obvious from this plot, the dispersion decreases with increasing temperature; i.e., the

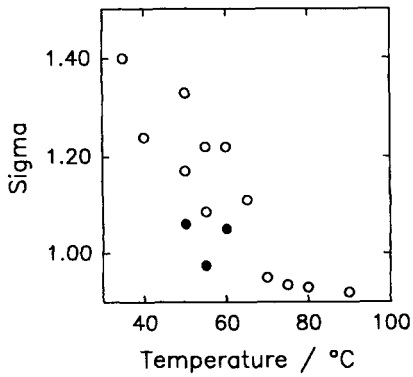

Figure 10. Thermal course of the dispersion parameter of isothermal measurement of SHG relaxations. Data referring to physically aged samples are depicted using filled circles.

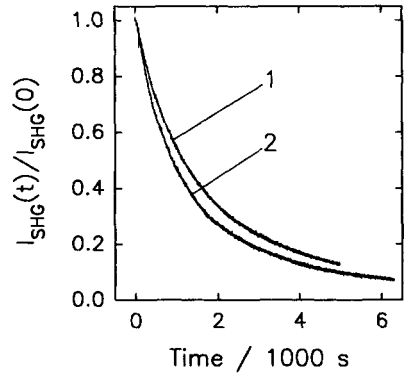

Figure 11. Normalized SHG decay data of a PEMA sample doped with 1 wt % DANS. The curves are for a sample aged at 50 °C for more than 1 h (1) and for a fresh sample (2).

relaxation approaches exponentiality. Within the temperature regime in which the matrix is rigid, the variance σ^2 of the rates is not expected to depend strongly on temperature. However, at temperatures sufficiently above T_G configurational averaging of the barriers (or rates) ultimately leads to an exponential decay. This behavior of "line narrowing" has been described previously by Richert[25] and Albrecht,[27] who examined the same class of matrix materials, albeit via probing the dynamics of an isomerization reaction. According to very recent measurements of Albrecht and Schäfer,[27] the necessary rigidity of the matrix for observing the low-temperature limit of σ should be reached at T_G - 50 K. In the present experiment, this limiting value of σ is obscured by physical aging effects, although an onset of saturation of σ at low temperatures is present (cf. Figure 10).

In order to get an idea of the extent of the impact of physical aging on the relaxation behavior, additional aging experiments were carried out in the following manner: Following the poling procedure, the samples were aged at the respective relaxation temperature for a period of time corresponding to the overall relaxation time at this temperature without previous aging. Data gained from this method are depicted in Figures 10 and 12 using filled dots. Figure 11 shows a comparison of some typical traces of SHG data in this context. The following conclusions can be drawn from these experiments: Physical aging reduces the mean velocity and dispersion of the process, as expected qualitatively from the generally accepted free-volume approach.[28] In terms of the applied model the Gaussian distribution is compressed and shifted to lower mean energies; i.e., mainly the fast processes are suppressed due to aging. Bearing this notion in mind, an estimation of the saturation temperature of the σ parameter cannot be extracted from the present set of data.

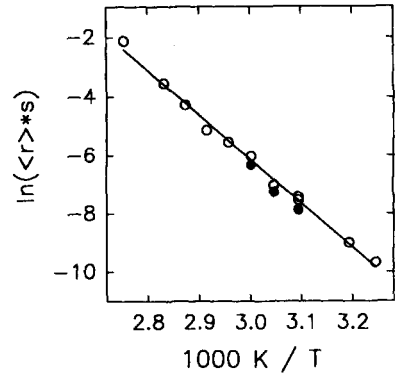

Figure 12. Arrhenius plot of the mean rate of isothermal SHG relaxation of a PEMA sample doped with 1 wt % DANS. Data of samples subject to physical aging are marked by filled circles.

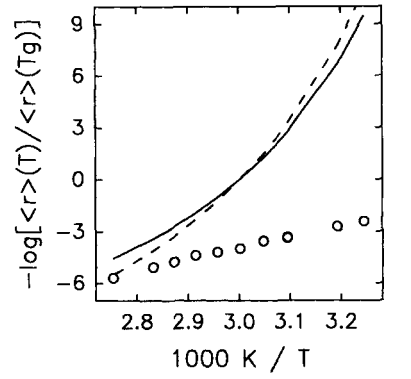

Figure 13. Temperature dependence of the mean rate of dopant reorientation within the range $T_G \pm 30$ K of a PEMA sample doped with 1 wt % DANS. The solid curve refers to a fit according to the WLF equation using[11] $C_1 = 14$ and $C_2 = 62$ °C; the dashed curve refers to $C_1 = 17.6$ and $C_2 = 65.5$ °C as WLF parameters.[28]

Increasing experimental difficulties appeared when expanding the duration of a single measurement to a time scale of more than 10 h. This is due to signal instabilities arising from base-line drifts and signal fluctuations which are believed to be caused by intrinsic charge diffusion. Therefore, no more experiments below T_G - 30 K were carried out. No aging effects could be seen at temperatures above 60 °C, which agrees with $T_G = 60$ °C as determined via DSC. Corresponding results are also gained by the long-term poling experiments described in section 4. Physical aging turned out to be fully reversible by the applied thermal erase (tested separately via reproducible SHG decays at 60 °C right after each aging experiment).

Figure 12 represents an Arrhenius plot of the mean rate. Even if aging effects are considered, it is evident that the temperature-dependent SHG relaxation of DANS in PEMA clearly follows an Arrhenius-like behavior with an activation energy of 126 kJ/mol. The observation coincides with that of King and Singer[12] obtained for a comparable PMMA guest/host system. Figure 13 shows the same result from a different point of view by presenting the deviation of our data from the well-known WLF approach:[29]

$$\log(\langle\tau\rangle/\langle\tau\rangle_G) = \frac{-C_1(T - T_G)}{C_2 + (T - T_G)} \qquad (9)$$

where $C_{1,2}$ denote the empirical WLF constants, $\langle\tau\rangle$ is the mean relaxation time, and $\langle\tau\rangle_G$ refers to $\langle\tau\rangle$ at $T = T_G$. The solid and dotted lines represent the expected polymer behavior according to different sources in the literature.[10,30] The course of these lines is generally accepted to be valid for temperatures beyond T_G. The experimental result of

our investigation clearly implies a temperature-dependent decoupling of dopant motion from the behavior of the polymer; i.e., in this case the chromophore does not seem to reflect the bulk polymer dynamics. Our present results point toward a dopant mobility which is mainly controlled via more localized matrix motions. Such local modes might be based on noncooperative movements of a single chain segment. The mobility of the ethyl side chain, which is assumed to cause the β-relaxation in PEMA,[10] might also contribute. A probably quite complex temperature-dependent participation of single localized processes thus might be responsible for the macroscopically observed reorientation of the chromophores at sub-T_G temperatures. Such a decoupling from the host dynamics might also be responsible for the relaxation patterns of the average chromophore orientation which comply with a Gaussian density of barriers and are thus atypical for a bulk relaxation of amorphous materials. According to dielectric measurements, the bulk relaxation, i.e., the α-process of PEMA, is more similar to a KWW behavior.[10] At elevated temperatures the α-motion gradually gains importance. It will be of further interest to examine to which extent an Arrhenius-like thermal course of the mean rate in the temperature range near T_G is a general feature. Although β-processes are notorious to follow an Arrhenius behavior,[30] they are too fast to be solely responsible for the present observation.

It is especially noteworthy that this experimental result is in significant conflict with that reported recently by Dhinojwala and co-workers.[10] In their report the same polymer (apart from a different molecular weight) doped with 2 wt % Disperse red (similar to DANS in size and SHG activity) was investigated. Both systems should be comparable due to the equal glass transition temperatures. Based on combined results of dielectric measurements and SHG decay experiments in a similar range of temperatures, a directly polymer-controlled chromophore reorientation via α-relaxation was postulated by this group. In their study the mean time constants above T_G were found to follow a WLF behavior.

A straightforward comparison with our results cannot easily be done because their poling technique involved chrome gap electrodes and is thus quite different from that used in our experiments. As pointed out charge effects due to electrode material, focus effects, and the sample preparation are also critical factors which had not been stated explicitly by this group. We also do not observe the γ-effect in a way described by Dhinojwala. Data concerning the thermal course of their KWW β-values for the PEMA measurements are not reported either. If dopant reorientation in this material were mainly α-relaxation-controlled, one would at least expect a saturation of the β-parameter in the sub-T_G region similar to what they have observed using poly(isobutyl methacrylate) (PIBMA) as a host. This, however, would not match the thermal course of our dispersion parameter (cf. Figure 10). The time scales for the decays we have observed are more similar to the results of Goodson and Wang,[13] Hampsch et al.,[18] or Singer et al.[12]

6. Repoling after Incomplete Relaxation. Additionally a novel technique involving SHG was applied to the PEMA/DANS system. The basic idea here is to monitor the SHG recovery as a function of time upon reapplying the external field after a foregoing SHG relaxation scan. This experiment is then repeated for different extents of the relaxation prior to repoling. A straightforward comparability of the temporal pattern is achieved by normalizing each scan and inverting the

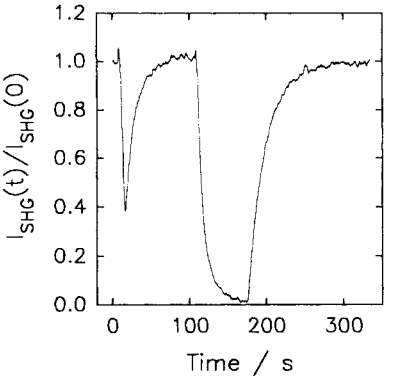

Figure 14. Raw data of a typical poling experiment following a partial relaxation of dopants for a PEMA sample doped with 1 wt % DANS at T = 90 °C.

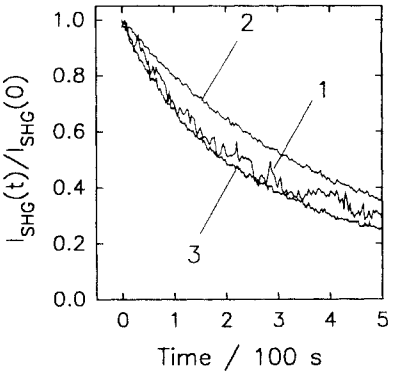

Figure 15. Normalized poling trace of a PEMA sample doped with 1 wt % DANS at T = 60 °C (=T_G). The SHG increase while poling is recorded directly after a relaxation extent of 10% (curve 1) and 80% (curve 2). Curve 3 refers to the normalized SHG decay trace.

recovery data. The basic result of such a series of experiments concerns the dependence of the SHG recovery pattern on the progress of the preceding SHG relaxation. Even if restricted to qualitative statements, this method should reveal whether or not the chromophores "memorize" their time scale of rotational mobility. Here again the conclusiveness of the measurement critically relies on the reproducibility of SHG relaxation data.

Preliminary experiments along these lines have indicated that the SHG relaxation kinetics were not affected by SHG recovery due to intermittent poling as long as the temperature was above T_G. At temperatures significantly below T_G aging effects again have to be considered. Figure 14 explains the basic procedure with the help of raw data of a typical SHG relaxation/recovery experiment at $T > T_G$. Figure 15 shows the results of a series of experiments done near T_G = 60 °C, whereas Figure 16 indicates the analogous measurement at T_G − 20 K. Similar measurements have also been done at 42, 70, 80, and 90 °C.

A feature always present at temperatures $T \geq T_G$ was that the normalized SHG recovery trace following a small degree of relaxation (typically 10%) revealed identical kinetics or at least comparable starting slopes. Increasing the extent of the preceding relaxation resulted in normalized poling processes of decreased velocity. Qualitatively, this behavior can be rationalized only if a chromophore at a particular site remembers its orientational response time on a time scale comparable to the mean overall relaxation time. In a simplified picture this means that a site which can be rotated easily toward the field direction can also reorient easily.

Within the picture of a heterogeneous (Gaussian) distribution of exponential responses with site-specific

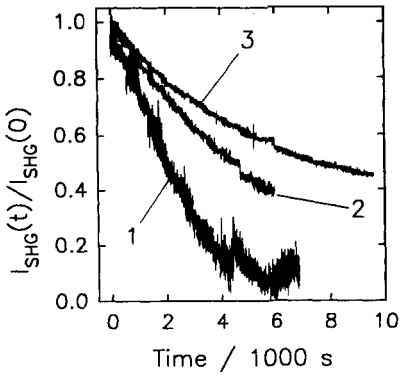

Figure 16. Normalized poling trace of a PEMA sample doped with 1 wt % DANS at T = 40 °C ($=T_G$ - 20 K). The SHG increase while poling is recorded directly after a relaxation extent of 10% (curve 1) and 60% (curve 2). Curve 3 refers to the normalized SHG decay trace.

time constants, the above finding for the SHG relaxation/recovery experiment can be rationalized in the following manner: At short times after removing the poling field those sites that are subject to fast response times dominate the SHG decay. As time proceeds the sites of more frustrated orientational freedom gradually gain importance. If the overall relaxation process is reverted at an intermediate stage be reapplying the poling field, two limiting cases can be envisaged: (i) The recovery signal is insensitive to the preceding relaxation history, or (ii) after applying the field again selectively those sites that had relaxed before are reoriented. The former case will apply whenever a site has no memory regarding its particular time constant or if relaxation and poling probe different subensembles of the chromophores. In the latter case, repoling after only a short preceding relaxation will be accelerated compared to repoling after a complete relaxation; i.e., relaxation and subsequent recovery time scales are correlated quantities. Qualitatively this has been observed. However, the data quality of this experiment is insufficient to quantify these correlations in terms of the fit parameters $\langle r \rangle$ and σ.

Summary and Conclusions

In this study we have presented a set of temperature-dependent SHG relaxation measurements covering the range T_G - 30 K to T_G + 30 K of the system PEMA doped with 1 wt % DANS. Using a novel cell design for electrode poling in connection with comparatively weak poling fields and a rapid data sampling technique, a high data quality was achieved. By varying many experimental parameters, we were able to find sample preparation and detection techniques at which we obtain reproducibilities on a level which is appropriate for a sensible decay pattern analysis. We have clear evidence that the dopant–dopant interactions in PEMA systems containing ≤1 wt % DANS can be neglected with respect to the decay kinetics. When investigating the commonly observed switching effects upon removing the poling field, it turned out that normalized decay kinetics are not affected as long as a limit of about 10% effect contribution in either direction is not exceeded. In view of the sensitivity to illumination at 300–450 nm and to thermal treatment, we postulate that these effects are due to space charges. The fast initial response observed by us cannot be explained solely by the similar so-called γ-effects recently mentioned by other authors.[10,14] Examination of electrode charge injection by measuring the cell current leads to the conclusion that ITO as an electrode material causes significant charge injection even when working at low fields. In the temperature regime $T \geq T_G$ this had no effect on the observed kinetics.

The SHG relaxation data were analyzed in terms of site-specific energy barriers subject to a heterogeneous Gaussian distribution, which allows us to quantify both mean rate and dispersion of the ensemble-averaged relaxation. The mean rate follows an Arrhenius-like behavior, implying that the dopant relaxation deviates significantly from the polymer behavior (cf. α-relaxation) which is roughly represented by the WLF approach. This decoupling of the guest molecules from the bulk rotational mobility is also emphasized by the dispersion parameter σ and its temperature dependence. Using a novel repoling technique characterized by dopant realignment of only partially relaxed samples, a more detailed insight into the correlation effects of SHG relaxation and recovery was possible. We observed a gradually decreasing mean rate of poling with an increasing degree of previous relaxation. Differences in the mean poling rate with respect to the mean relaxation rate, which are obvious when data of experiments at $T \geq T_G$ are compared with corresponding data from the sub-T_G region, were interpreted in terms of matrix mobility.

Unfortunately, a quantitative comparison of our results to literature data is hampered by differences in the experimental details. In general, however, this type of measurement selectively probes the rotational diffusion of the tracer molecules, i.e., of the hyperpolarizable chromophore. Tracer diffusion coefficients are also accessible via forced Rayleigh scattering[32,33] and by depolarization of optical labels.[34,35] From such experiments it is known that the decoupling of tracer diffusion from the bulk rotational motion depends critically on the size of the dopant; in the limit of large tracers the decoupling effect vanishes. Therefore, in cases where one is interested in a long-term stability of the second-harmonic optical activity, bulkier dopants should be preferred.

On the basis of highly reproducible results, an investigation of other polymers, especially PIBMA assumed to show only α-relaxation,[31] will be the subject of further research. Electrode modifications aimed at reducing charge injection would also be helpful with respect to improved poling experiments. Furthermore, a complete investigation of the materials under study by means of dielectric relaxation spectroscopy covering a temperature range similar to that of the corresponding SHG experiments is in progress.

Acknowledgment. We gratefully thank Philipps University of Marburg for supporting this work by a Ph.D. scholarship and U. Albrecht for his support in the field of software development. We also thank E. O. Göbel (Department of Physics, Marburg University) for providing the Nd:YAG laser.

References and Notes

(1) Prasad, P. N.; Williams, D. J. *Introduction to Nonlinear Optical Effects in Molecules and Polymers*; Wiley-Interscience: New York, 1991.
(2) Chemla, D. S., Zyss, J., Eds. *Nonlinear Optical Properties of Organic Molecules and Crystals*; Academic Press: New York, 1987.
(3) Eich, M.; Bjorklund, G. C.; Yoon, D. Y. *Polym. Adv. Technol.* **1990**, *1*, 189.
(4) Meredith, G. R.; VanDusen, J. G.; Williams, D. J. *Macromolecules* **1982**, *15*, 1385.
(5) Williams, D. J. *Angew. Chem.* **1984**, *96*, 637.
(6) Singer, K. D. *Polym. Prepr. (Am. Chem. Soc., Div. Polym. Chem.)* **1992**, *33*, 396.
(7) Miller, R. D.; Burland, D. M.; Lee, V.; Moylen, C. M.; Staehelin, M.; Twieg, R. J.; Volksen, W.; Walsh, C. A. Conference of the Polymers for microelectronics, Kawasaki, Japan, 1993, p 257.

(8) Staehelin, M.; Burland, D. M.; Ebert, M.; Miller, R. D.; Smith, B. A.; Twieg, R. J. Volksen, W.; Walsh, C. A. *Appl. Phys. Lett.* **1992**, *61*, 1626.
(9) Shen, Y. R. *Principles of Nonlinear Optics*; Wiley-Interscience: New York, 1984.
(10) Dhinojwala, A.; Wong, G. K.; Torkelson, J. M. *Macromolecules* **1993**, *26*, 5943.
(11) Hampsch, H. L.; Yang, J.; Wong, G. K.; Torkelson, J. M. *Macromolecules* **1988**, *21*, 528; **1990**, *23*, 3648.
(12) Singer, K. D.; King, L. A. *Polym. Prepr. (Am. Chem. Soc., Div. Polym. Chem.)* **1991**, *32*, 98; *J. Appl. Phys.* **1991**, *70*, 3251.
(13) Goodson, T.; Wang, C. H. *Macromolecules* **1993**, *26*, 1837.
(14) Dhinojwala, A.; Wong, G. K.; Torkelson, J. M. *Macromolecules* **1992**, *25*, 7395.
(15) Walsh, C. A.; Burland, D. M.; Lee, V. Y.; Miller, R. D.; Smith, B. A.; Twieg, R. J.; Volksen, W. *Macromolecules* **1993**, *26*, 3720.
(16) Teraoka, I.; Jungbauer, D.; Reck, B.; Yoon, D. Y.; Twieg, R.; Willson, C. G. *Appl. Phys.* **1991**, *69*, 2568.
(17) Williams, G.; Watts, D. C. *Trans. Faraday Soc.* **1970**, *66*, 80. Kohlrausch, R. *Ann. Phys. (Leipzig)* **1847**, *12*, 393.
(18) Hampsch, H. L.; Yang, J.; Wong, G. K.; Torkelson, J. M. *Macromolecules* **1990**, *23*, 3640.
(19) Man, H. T.; Yoon, H. N. *Adv. Mater.* **1992**, *4*, 159.
(20) Hampsch, H. L.; Yang, J.; Wong, G. K.; Torkelson, J. M. *Polym. Commun.* **1989**, *30*, 40.
(21) Schüssler, S. Thesis, Philipps Universität Marburg, FRG, 1991.
(22) Vestweber, H.; Greiner, A.; Lemmer, U.; Mahrt, R. F.; Richert, R.; Heitz, W.; Bässler, H. *Adv. Mater.* **1992**, *4*, 661.
(23) Richert, R. In *Optical Techniques to Characterize Polymer Systems*; Bässler, H., Ed.; Elsevier: Amsterdam, The Netherlands, 1989.
(24) Richert, R. *Macromolecules* **1988**, *21*, 923.
(25) Richert, R. *Mol. Cryst. Liq. Cryst.* **1990**, *183*, 283; *Chem. Phys.* **1988**, *122*, 455.
(26) Palmer, R. G.; Stein, D. L.; Abrahams, E.; Anderson, P. W. *Phys. Rev. Lett.* **1984**, *53*, 958.
(27) Albrecht, U.; Schäfer, H.; Richert, R. *Chem. Phys.* **1984**, *182*, 61.
(28) Doolittle, A. K. *J. Appl. Phys.* **1951**, *22*, 1471.
(29) Williams, M. L.; Landel, R. F.; Ferry, J. D. *J. Am. Chem. Soc.* **1955**, *77*, 3701.
(30) Aklonis, J. J.; MacKnight, W. J. *Introduction to Polymer Viscoelasticity*; Wiley-Interscience: New York, 1983.
(31) Ishida, Y.; Yamafuij, K. *Kolloid Z.* **1961**, *177*, 97.
(32) Ehlich, D.; Sillescu, H. *Macromolecules* **1990**, *23*, 1600.
(33) Sillescu, H.; Bartsch, E. In *Disorder Effects on Relaxation Processes*; Richert, R., Blumen, A., Eds.; Springer: Berlin, 1994.
(34) Hyde, P. D.; Ediger, M. D. *Macromolecules* **1989**, *22*, 1510.
(35) Cicerone, M. T.; Ediger, M. D. *J. Chem. Phys.* **1992**, *97*, 2156.